

Probing hot and dense matter in heavy ion collisions via neutral mesons and photons with the ALICE detector at the LHC

Astrid Morreale

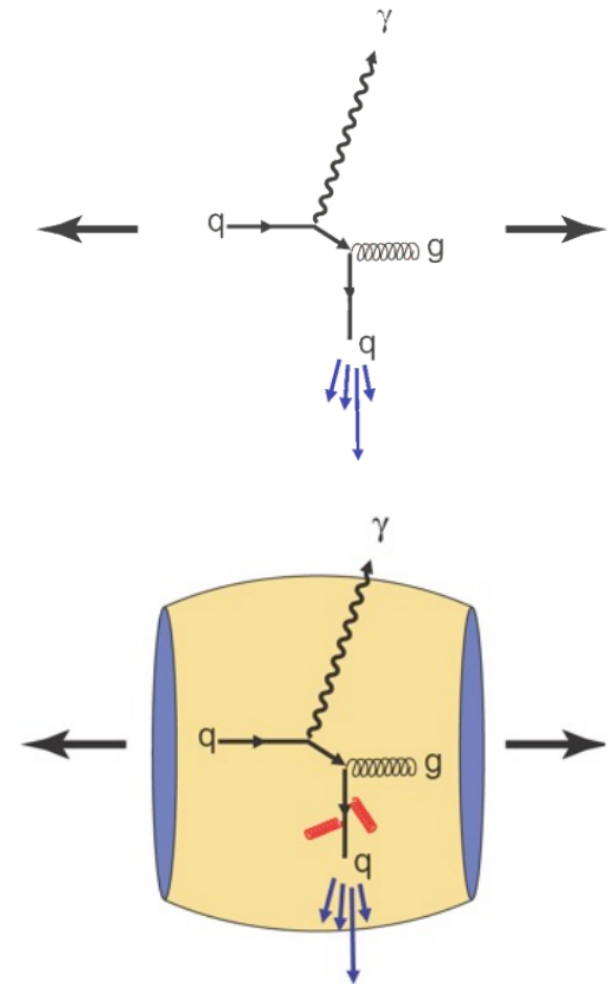
SUBATECH

September 17 2014

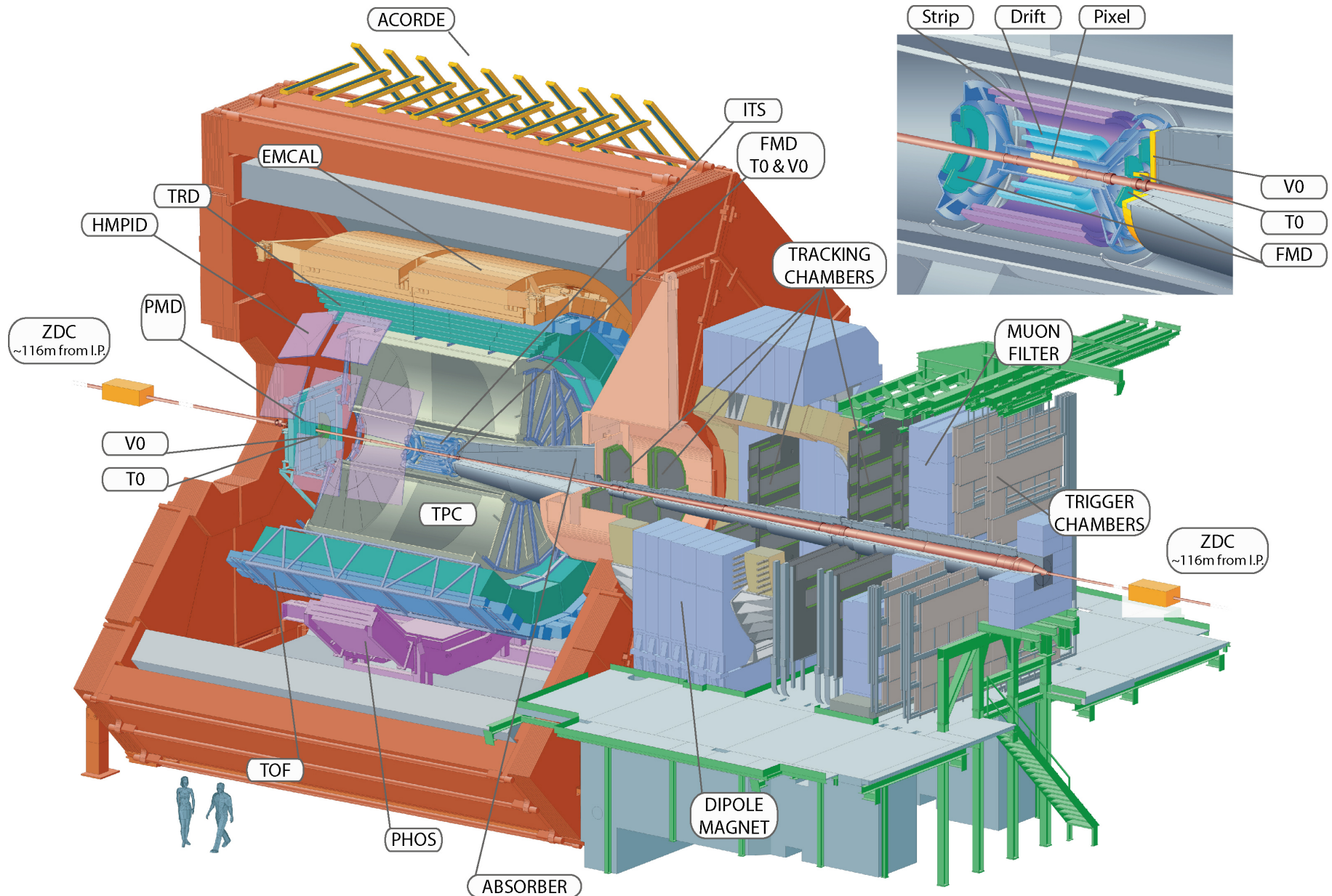
Rencontres QGP-France 2014

- They are the most abundant particles produced in HI, pp collisions
- The analysis used to detect them are similar and complementary (one is the background of the other)
- Their birth occurs at different stages of the collisions.
- In pp collisions: photons are produced at the initial stage of collisions while hadrons are produced from parton fragmentation in the QCD vacuum.
- The bulk of the particles created in HI collisions come from strongly interacting partons that escape at the end of the fireball's evolution. Parton fragmentation is modified by the presence of strongly interacting medium.
- Photons interact electromagnetically and they can escape the fireball during all collision stages.
- Direct photon at high p_T probes binary NN scaling, while at low p_T , direct photon excess is expected from thermal radiation of the QGP.

These effects can be observed via inclusive spectra modifications and hadron-hadron correlations.



- Detection.
- π^0 production in pp collisions.
- π^0 production in Pb-Pb collisions $\longrightarrow R_{AA}$
- η production in pp and Pb-Pb collisions.
- Latest results on direct photons in Pb-Pb collisions.
- Conclusions



Detectors relevant for this presentation: PHOS, EMCAL and ITS, TPC

- PHOS calorimeter:

PbWO4 crystal, 3 modules at 4.6 m from ALICE's IP.

$$|\eta| < 0.13, 260^\circ < \phi < 320^\circ$$

$$\frac{\sigma_{E(\text{GeV})}}{E} = \frac{0.018}{E} \oplus \frac{0.033}{\sqrt{E}} \oplus 0.011$$

- EMCal calorimeter:

77 layers 1.4 mm lead + 1.7 mm scintillator

10 modules at 4.4 m from ALICE IP.

$$|\eta| < 0.7, 80^\circ < \phi < 180^\circ.$$

$$\frac{\sigma_{E(\text{GeV})}}{E} = \frac{0.05}{E} \oplus \frac{0.1 \pm 0.04}{\sqrt{E}} \oplus 0.017$$

- Photon Conversion Method (PCM):

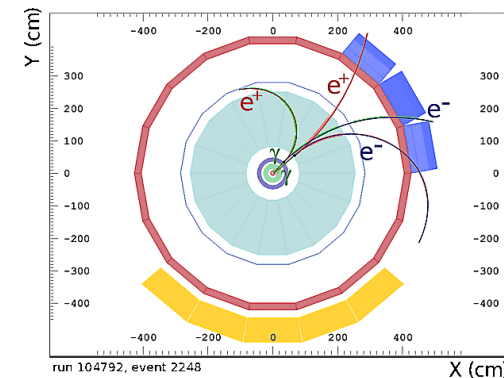
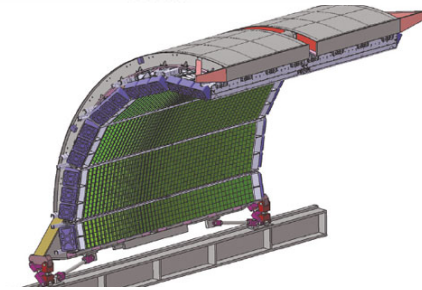
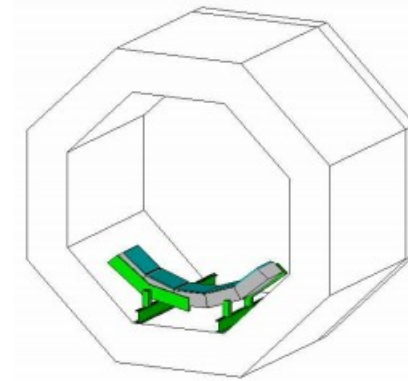
Photon conversion in detector material

ITS and TPC ($X/X_0 = 11.4 \pm 0.5_{\text{sys}} \%$)

$$|\eta| < 0.9, 0^\circ < \phi < 360^\circ.$$

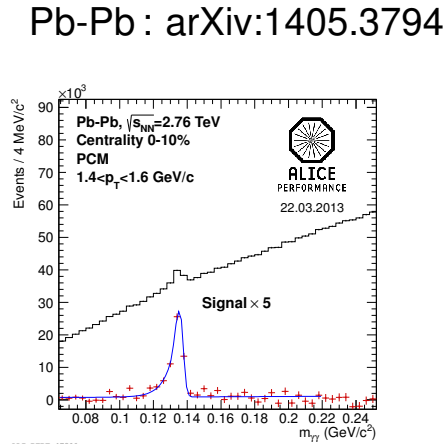
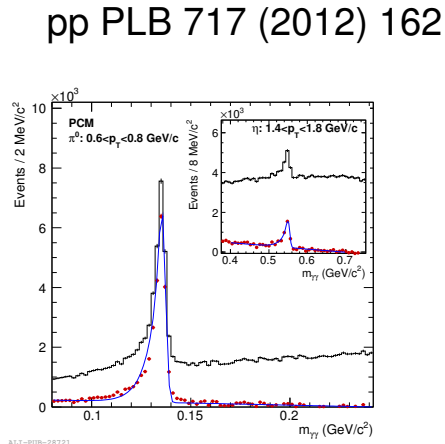
$$\sigma_R < 2 \text{ cm}, \sigma_Z < 1.5 \text{ cm}, \sigma_\phi < 7 \text{ mrad}$$

Conversion probability is small but it is compensated by a wide acceptance.

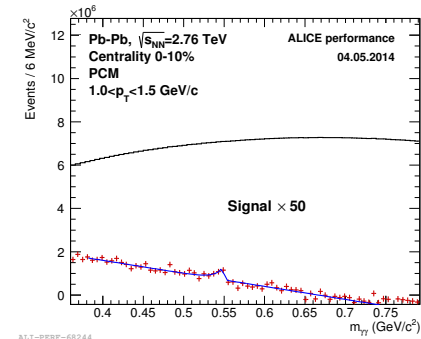


All three methods have completely different systematic uncertainties. Their combined measurements of photon observables is important to minimize biases.

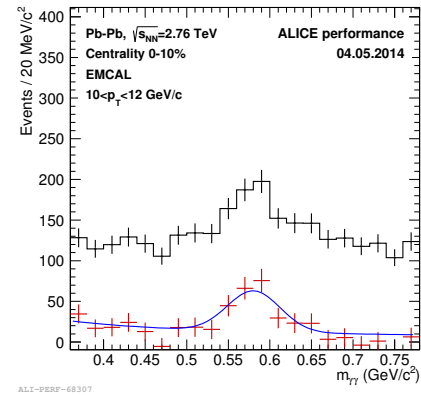
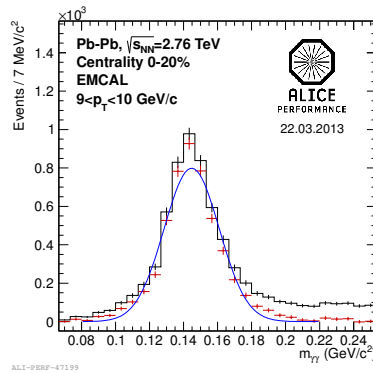
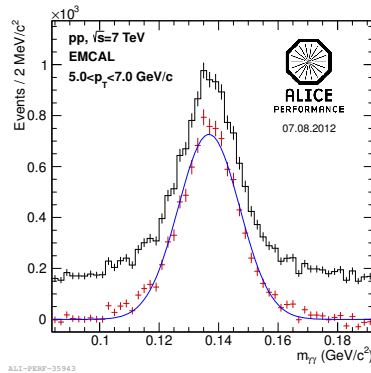
PCM



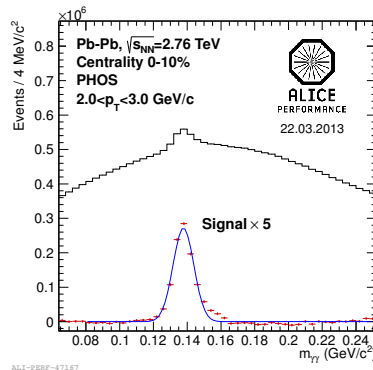
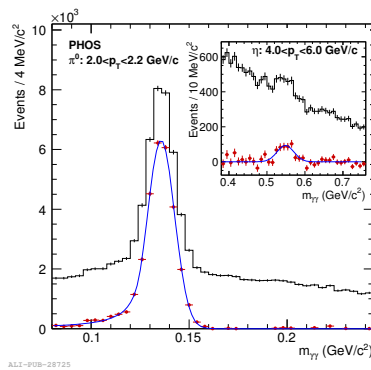
Pb-Pb (η meson)



EMCAL



PHOS

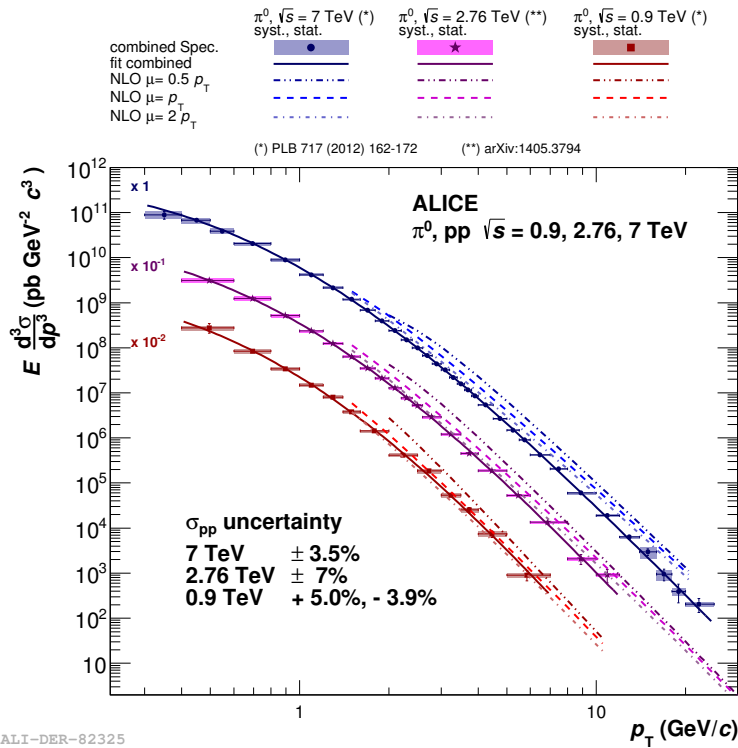


$$M_{\gamma\gamma} = \sqrt{2E_{\gamma_1}E_{\gamma_2}(1 - \cos\theta_{\gamma_1\gamma_2})}$$

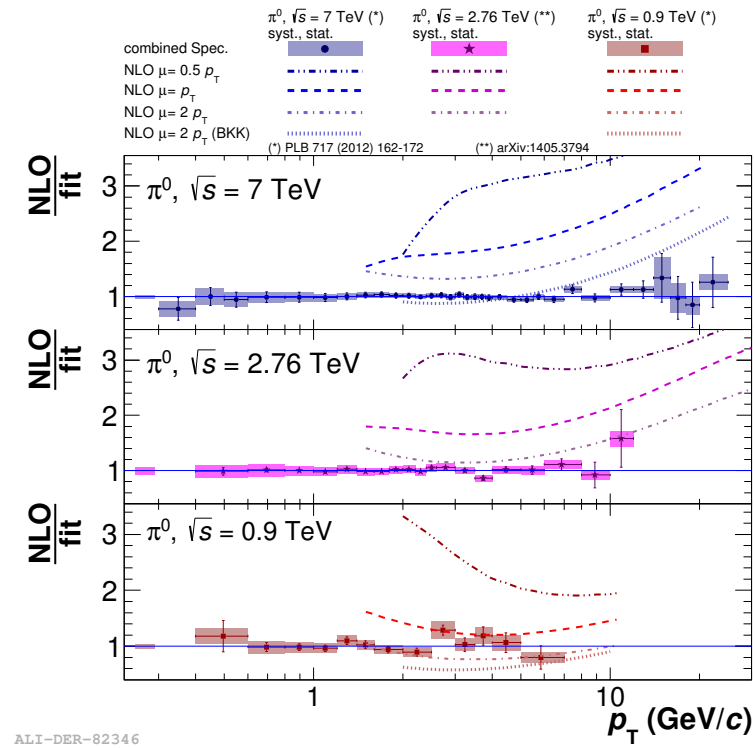
Wide p_T range accessible with all detectors.

All measurements are complementary.

π^0 invariant yields in pp



ALI-DER-82325

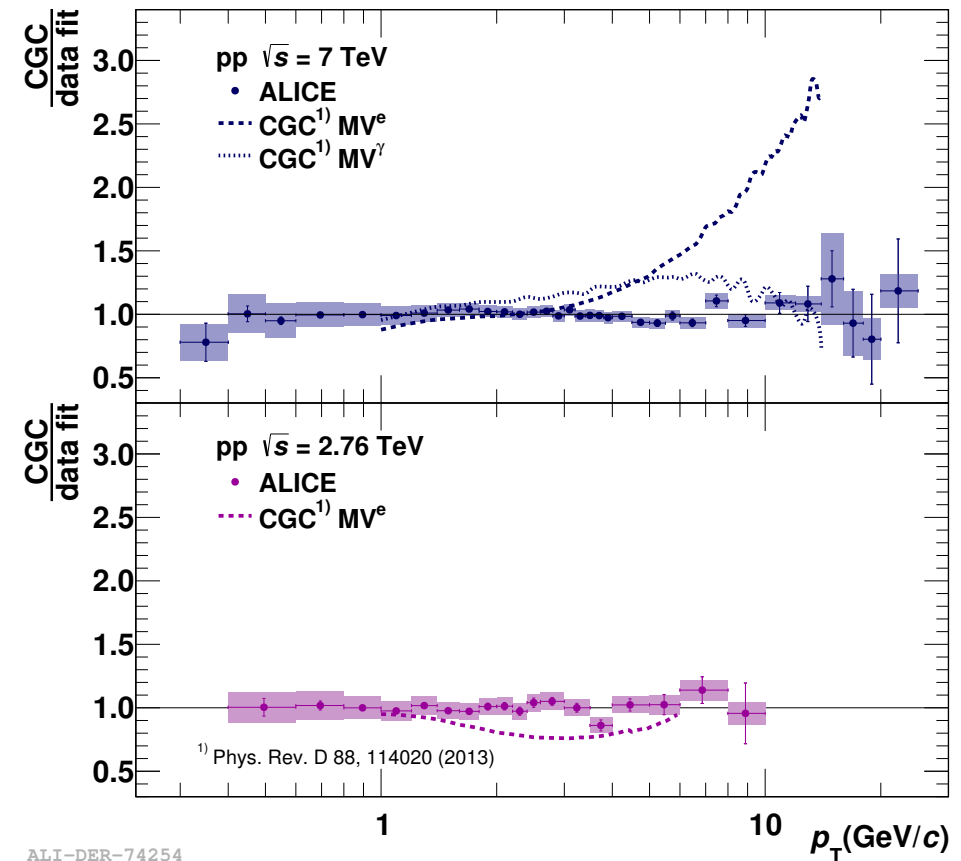
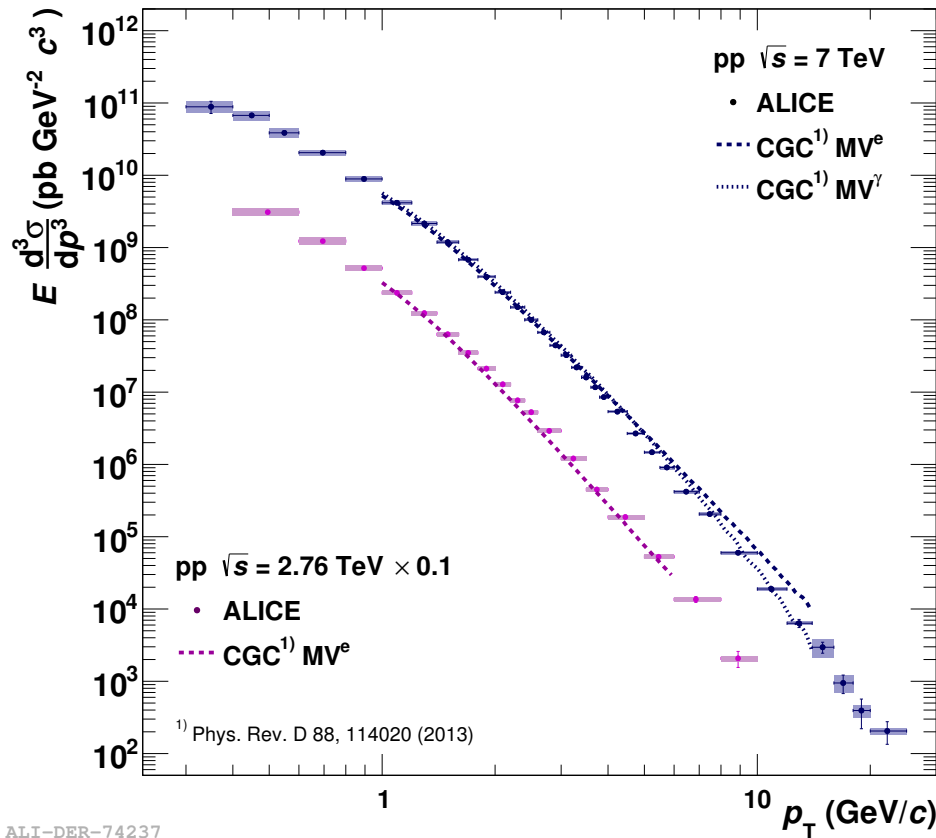


ALI-DER-82346

- Figure: Invariant yields at three \sqrt{s}
- Power law dependence at high p_T
 $n = 6.0 \pm 0.1$ ($\sqrt{s} = 2.76$ TeV)
 to be compared to $n = 8.22 \pm 0.1$ at RHIC ($\sqrt{s} = 0.2$ TeV)

- Figure: The current NLO pQCD calculations fail to describe π^0 production at $\sqrt{s} = 2.76$ TeV and 7 TeV.
- PDF: CTEQ6M5, fragmentation functions: DSS and BKK (π^0), AESS(η)

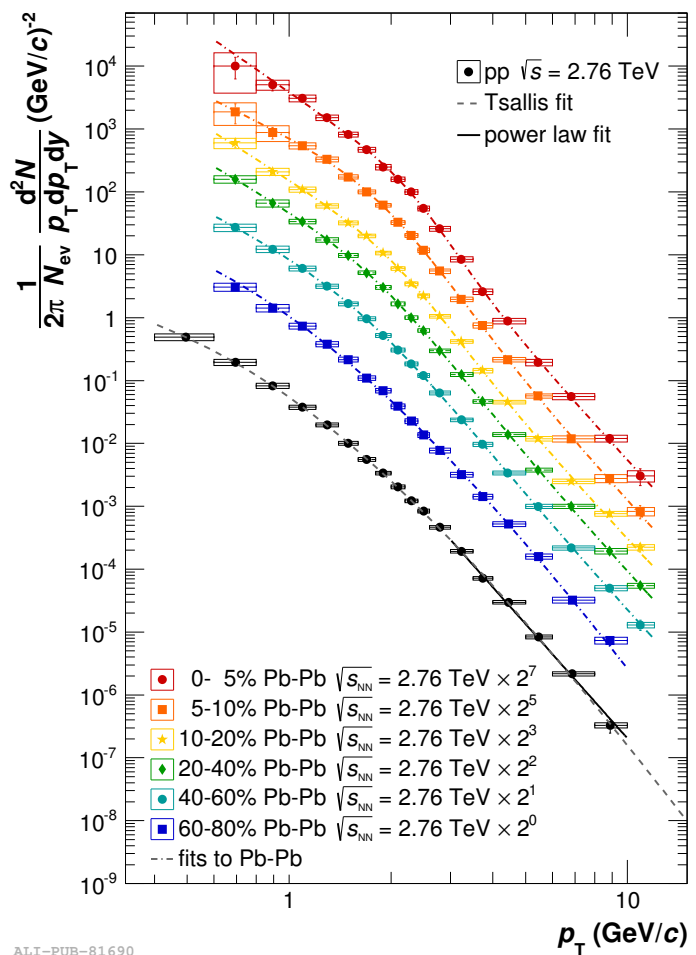
pp $\sqrt{s} = 0.9, 7$ TeV: PLB 717 (2012) 162; $\sqrt{s} = 2.76$ TeV: arXiv:1405.3794



Model describes ALICE data in the p_T region of 1-10 GeV/c

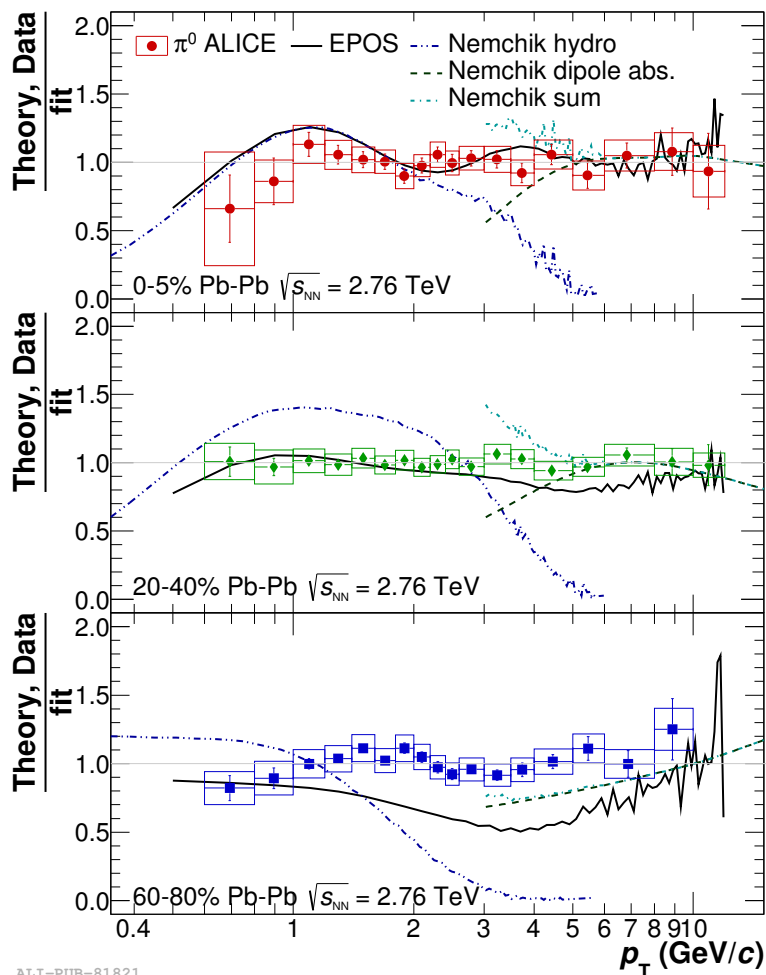
T. Lappi, H.Mäntysaari, Phys. Rev. D88 (2013) 114020

π^0 invariant yields in Pb-Pb



Left figure: π^0 yields measured in six centrality classes. (arXiv:1405.3794)

- EPOS: Phys. Rev. C85, 064907 (2012):
 Low p_T : Hydrodynamic flow
 High p_T : Energy loss of string segments



Right figure: Model comparisons

- Nemchik (PRC86, 054904, 2012):
 Low p_T : Hydrodynamic description
 High p_T : Color dipole absorption

ALI-PUB-81690

ALI-PUB-81821

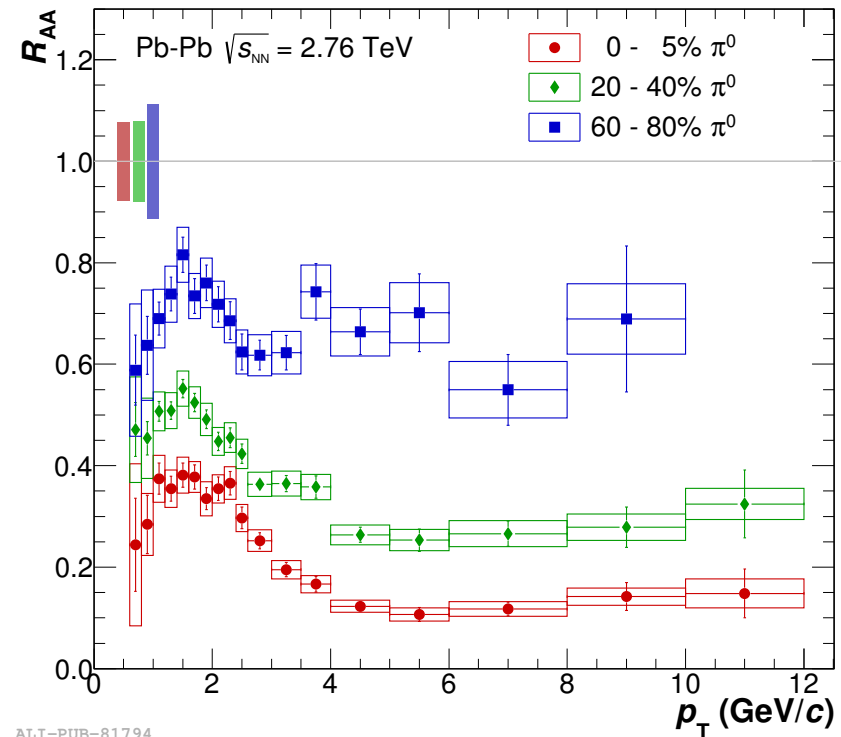
$$- R_{AA}(p_T) = \frac{1}{N_{coll}} \frac{dN_{AA}/dp_T}{dN_{pp}/dp_T}$$

- Measured to quantify nuclear effects in A-A collisions
- Production in A-A is compared to production in scaled pp collisions
- Number of binary nucleon-nucleon collisions (N_{coll}) is taken from Glauber Monte Carlo simulations.

- R_{AA} contains both initial and final state effects.

Initial state: i.e. Cronin, nuclear shadowing.

Final state: Jet quenching



- Figure: π^0 R_{AA} in three centrality classes.

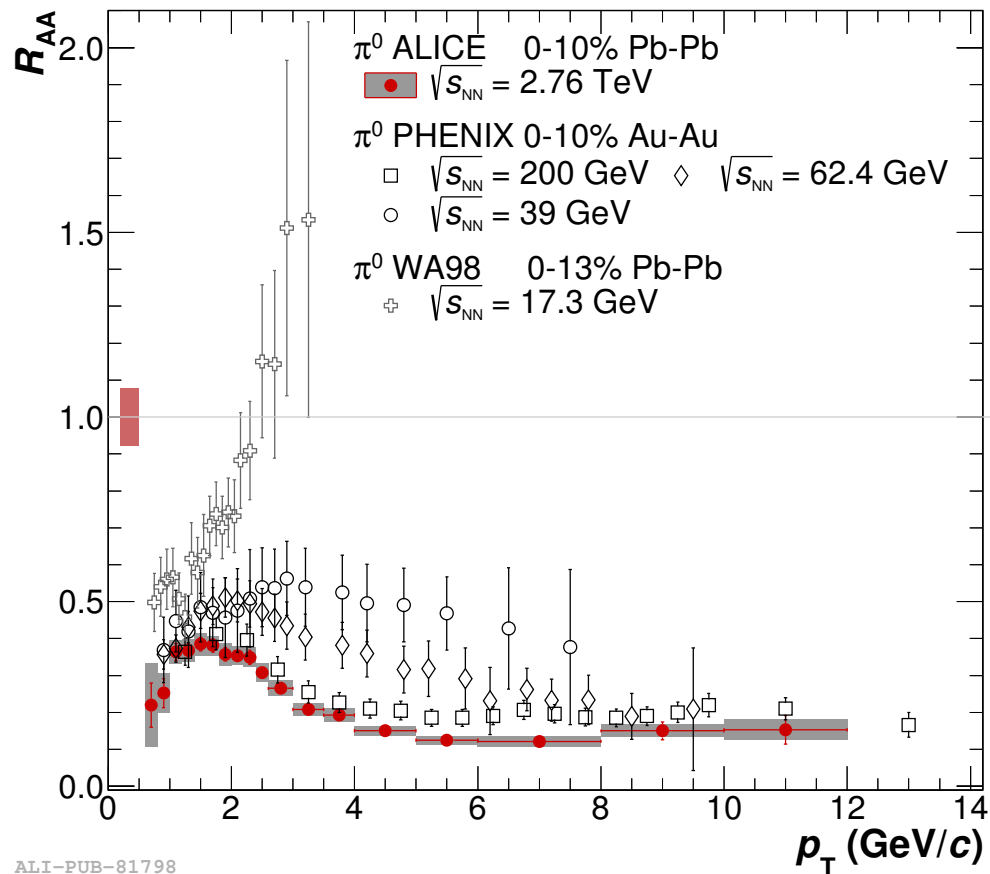
Large π^0 suppression in central Pb-Pb collisions.

60-80%: $R_{AA} \sim 0.6$ for $p_T > 6$ GeV/c

0-5% $R_{AA} \sim 0.1$ for $p_T > 6$ GeV/c

pp and Pb-Pb $\sqrt{s_{NN}} = 2.76$ TeV: arXiv:1405.3794

π^0 R_{AA} , in Pb-Pb collisions at $\sqrt{s_{NN}} = 2.76$ TeV for the 0 – 10% class in comparison to corresponding measurements at lower energies.



- π^0 R_{AA} at LHC lower than at RHIC
- Similarities observed between the R_{AA} shape at $\sqrt{s_{NN}} = 2.76$ TeV and $\sqrt{s_{NN}} = 200$ GeV.
- Onset of suppression between $\sqrt{s_{NN}} = 17.3$ GeV and $\sqrt{s_{NN}} = 39$ GeV

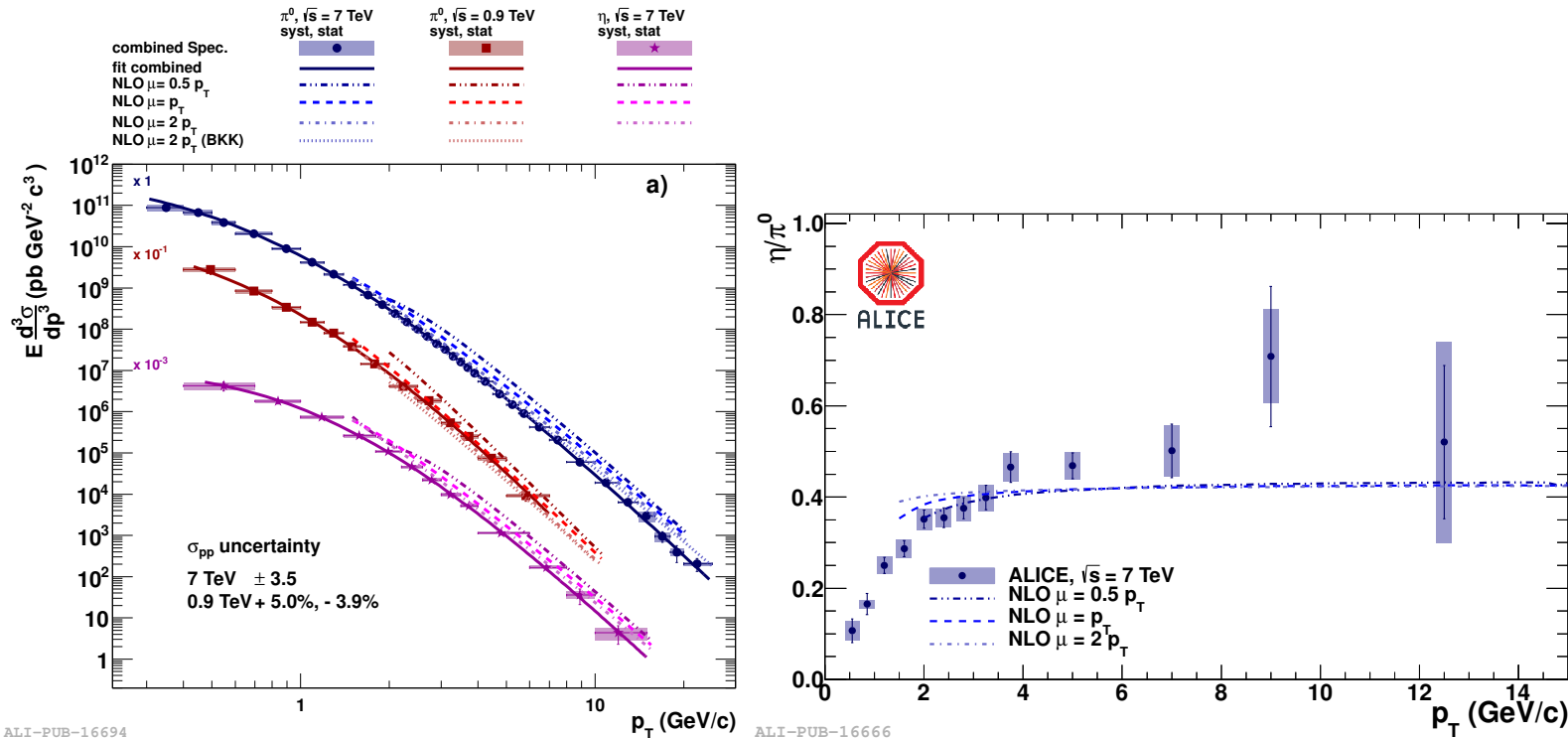
ALICE: arXiv:1405.3794.
PHENIX: PRL109,152301 (2012), 1204.1526
PHENIX: PRL101, 232301 (2008), 0801.4020
WA98: PRL100, 242301 (2008), 0708.2630

η Meson

The η meson has different flavor structure, partonic subprocess mix.

It has a larger opening angle thus merging of photons occurs at higher p_T values.

Suppression pattern in HI collisions seen for π^0 is expected also for η .



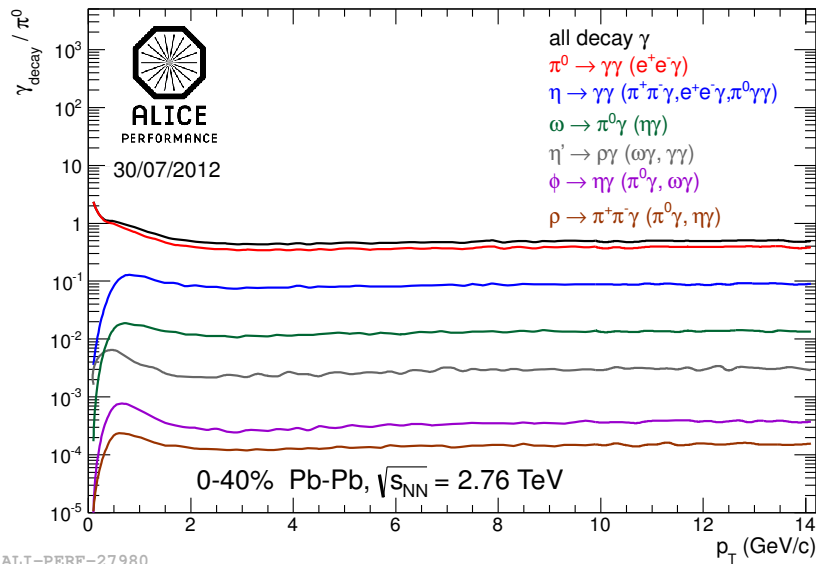
η in pp at $\sqrt{s_{NN}} = 7 \text{ TeV}$. Left figure: Invariant yields. Right figure η/π^0 ratio

Reliable knowledge of the production η is also needed as they constitute the second most important source of background after π^0 for measurements of single electrons from heavy-quark decays, dielectrons and direct photons.

Direct γ

Subtraction Method:

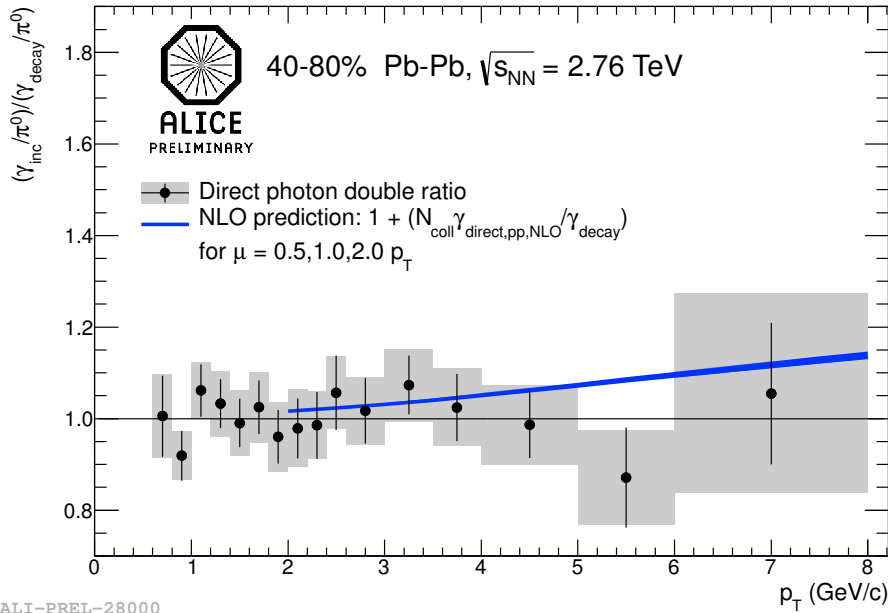
$$\gamma_{direct} = \gamma_{inc} - \gamma_{decay} = \left(1 - \frac{\gamma_{decay}}{\gamma_{inc}}\right) \gamma_{inc} = \left(1 - \frac{1}{R_\gamma}\right) \gamma_{inc}$$



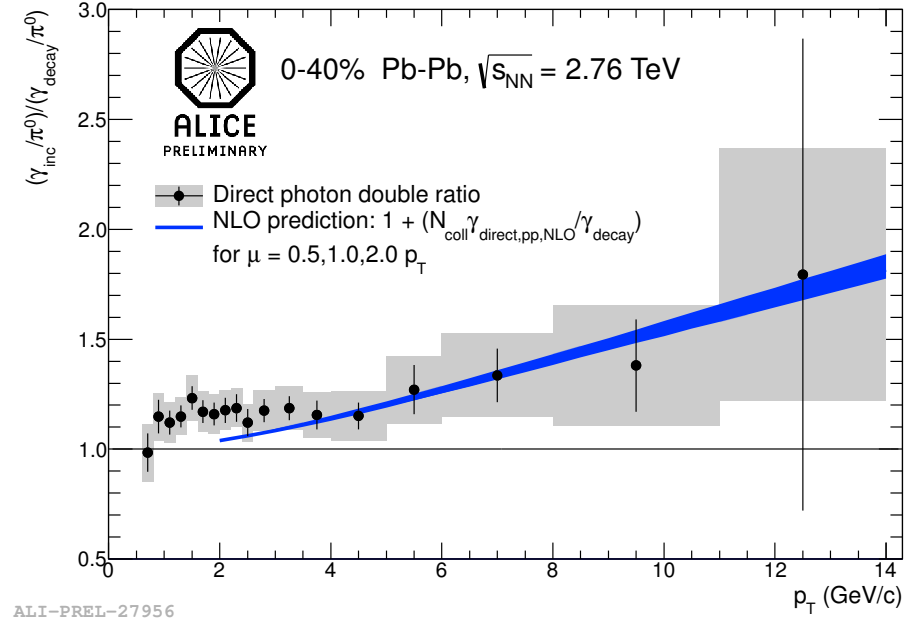
- γ_{inc} : inclusive photons
- γ_{decay} : decay photons calculated using cocktail based on measured π^0 spectrum with photon decay branching (figure)
- m_T scaling is assumed for unmeasured sources (η , ω , η' etc).

Double ratio: $R_\gamma = \frac{\gamma_{inc}}{\pi^0} / \frac{\gamma_{decay}}{\pi^0_{param}}$

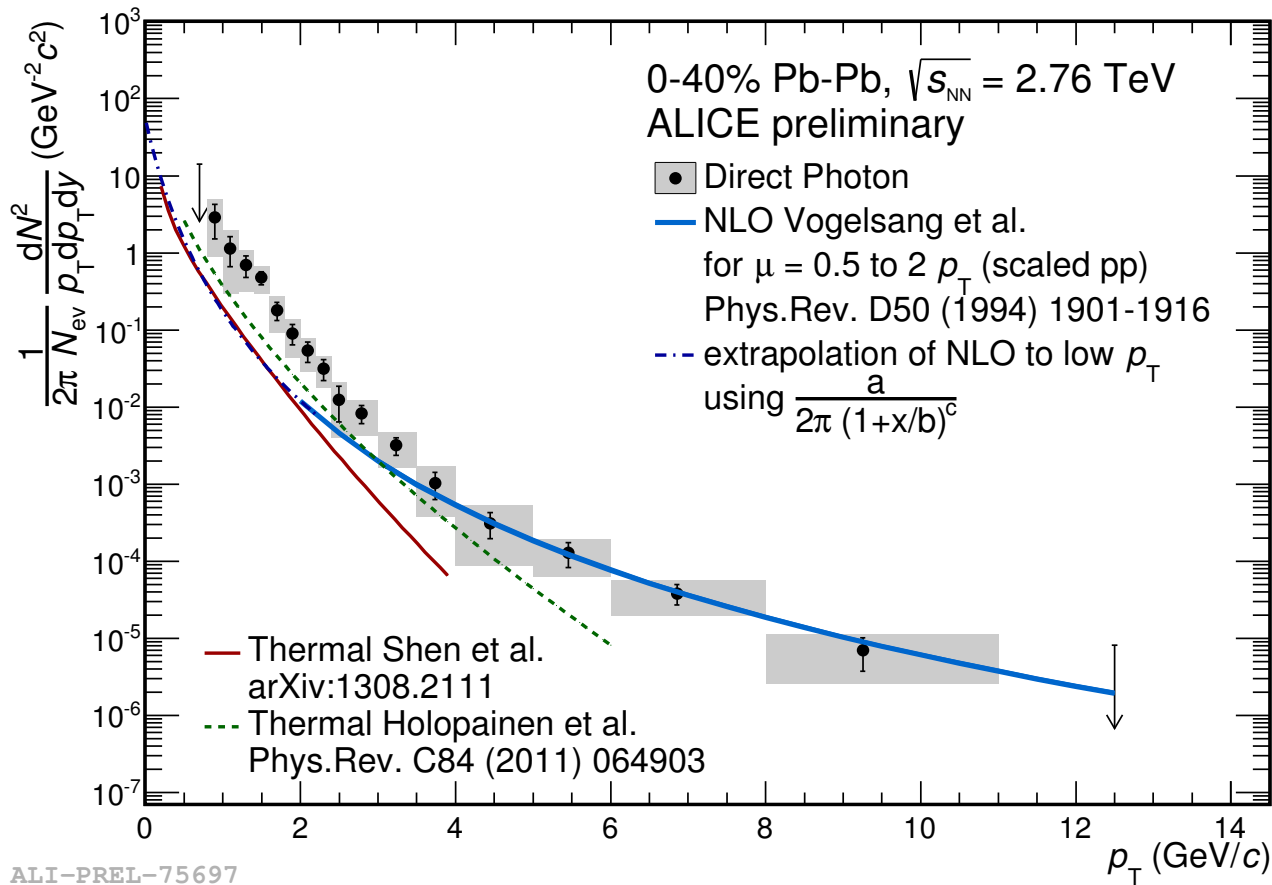
- R_γ greater than one indicates the observation of a direct photon signal.
- $\frac{\gamma_{inc}}{\pi^0}$: Inclusive photon spectrum per π^0
- $\frac{\gamma_{decay}}{\pi^0_{param}}$: All decay photons per π^0



- Left figure: Peripheral collisions. As expected, do not indicate production excess.



- Right figure: Central collisions. At low p_T ($p_T < 4$ GeV/c), an excess of $20\% \pm 5\%^{stat} \pm 10\%^{syst}$ is observed.



- Figure: Direct photon spectrum for central Pb-Pb collisions.

Spectrum is derived from the double ratio by $\gamma_{direct} = (1 - 1/R_\gamma)\gamma_{inc}$

- Exponential slope of $T = 304 \pm 51$ stat+syst MeV.

- Current uncertainties do not allow to discriminate between predictions beyond 2σ

- π^0 invariant yields have been measured by ALICE in pp and in 6 centrality classes in Pb-Pb collisions.
- NLO pQCD calculations do not describe well π^0 production in pp collisions at higher center of mass energies ($\sqrt{s} = 2.76$ and 7 TeV).
- A suppression on the measured π^0 's R_{AA} is observed.

While the shape of R_{AA} is comparable between RHIC and LHC energies, at the LHC we see a stronger suppression \leftarrow energy dependence.

- Theoretical models concerning π^0 production in Pb-Pb collisions only partially describe ALICE data.
- Ongoing efforts to extend current π^0 measurements .
- Ongoing effort to have a combined PCM-EMCal η measurement.
- Direct photon R_γ and invariant yields have been measured with an exponential slope of $T = 304 \pm 51$ stat+syst MeV.